nature neuroscience

Neuronal ensembles sufficient for recovery sleep and the sedative actions of α_2 adrenergic agonists

Zhe Zhang[1,3], Valentina Ferretti[1,3], İlke Güntan[1], Alessandro Moro[1], Eleonora A Steinberg[1], Zhiwen Ye[1], Anna Y Zecharia[1], Xiao Yu[1], Alexei L Vyssotski[2], Stephen G Brickley[1], Raquel Yustos[1], Zoe E Pillidge[1], Edward C Harding[1], William Wisden[1] & Nicholas P Franks[1]

Do sedatives engage natural sleep pathways? It is usually assumed that anesthetic-induced sedation and loss of righting reflex (LORR) arise by influencing the same circuitry to lesser or greater extents. For the α2 adrenergic receptor agonist dexmedetomidine, we found that sedation and LORR were in fact distinct states, requiring different brain areas: the preoptic hypothalamic area and locus coeruleus (LC), respectively. Selective knockdown of α2A adrenergic receptors from the LC abolished dexmedetomidine-induced LORR, but not sedation. Instead, we found that dexmedetomidine-induced sedation resembled the deep recovery sleep that follows sleep deprivation. We used TetTag pharmacogenetics in mice to functionally mark neurons activated in the preoptic hypothalamus during dexmedetomidine-induced sedation or recovery sleep. The neuronal ensembles could then be selectively reactivated. In both cases, non-rapid eye movement sleep, with the accompanying drop in body temperature, was recapitulated. Thus, α2 adrenergic receptor–induced sedation and recovery sleep share hypothalamic circuitry sufficient for producing these behavioral states.

© 2015 Nature America, Inc. All rights reserved.

Sedatives target just a handful of receptors and ion channels[1,2]. But explaining how activating these receptors produces sedation presents a challenge[2]. In particular, do sedatives act at specific brain locations and circuitries or more widely? Some powerful sedatives, such as clonidine, guanfacine, xylazine and dexmedetomidine, are agonists at inhibitory metabotropic adrenergic α2 receptors. Among these, dexmedetomidine is being assessed as an alternative to benzodiazepines for sedating patients during intensive care[3]. It induces a state resembling non-rapid eye movement (NREM) sleep, with lowered body temperature and enhanced slow-wave activity in the neocortex[4–6].

At the circuit level it is unclear how α2 agonists induce sedation and loss of consciousness in humans or the presumed surrogate, LORR in animals[7]. The most popular proposal hinges on the selective inhibition by α2A (*Adra2a*) receptors, of noradrenergic neurons in the locus coeruleus (LC)[7–11]. These neurons fire during waking, fire less during sleep and their activity increases just before waking, suggesting that they promote wakefulness[12–14]. Although selectively stimulating LC neurons induces waking[15], the converse is not true: acutely inhibiting LC neurons does not produce strong sleep, even after 1 h of stimulation[15], an unexpected result if α2 agonists are supposed to acutely inhibit the LC to induce hypnosis. Moreover, dexmedetomidine still induces LORR in mice unable to synthesize noradrenalin (NA)[7,16,17], although, without the endogenous ligand, α2A-receptor responses elsewhere become hypersensitized in the long term[7,17], making interpretation of this observation difficult[7].

We hypothesized that the heavy, but arousable, nature of α2 agonist–induced sedation might be most similar to the NREM sleep experienced after sleep deprivation, so-called recovery sleep. In both cases, there is a strong urge to enter deep sleep. One place where these effects might come together is the preoptic (PO) hypothalamus. The PO area, a mixture of sleep-active, wake-active, temperature-sensitive and state-indifferent neurons[18–20], houses circuitry that initiates and/or maintains sleep[18,19,21–23] and regulates body temperature[18].

We first used siRNA knockdown, which established that, although dexmedetomidine-induced LORR depended on activating α2A receptors on LC neurons, sedation did not, suggesting that these states depend on different neuronal populations. We next explored whether the two types of deep sleep—the sedation imposed by dexmedetomidine and the recovery sleep following sleep deprivation, together with the accompanying drop in body temperature—required similar neural circuitry. For this, we combined TetTagging with DREADD pharmacogenetics (TetTag-DREADD)[24–26]. We 'tagged' neuronal ensembles in the PO hypothalamus that were activated during recovery sleep or dexmedetomidine-induced sedation, and then caused these tagged ensembles to be selectively reactivated using the hM_3D_q receptor and its ligand, clozapine-*N*-oxide (CNO)[27]. In both cases, reactivating the ensemble for sedation or recovery sleep produced sustained NREM sleep, together with a lower body temperature. We found that recovery sleep and α2 adrenergic receptor–induced sedation were not only similar behavioral states, but were both induced by activating similar neuronal populations in the PO hypothalamus.

RESULTS

Sedation and LORR require distinct neuronal populations

We examined dexmedetomidine's action at α2A receptors selectively in the LC, using acute knockdown of *Adra2a* transcripts, and

[1]Department of Life Sciences, Imperial College London, South Kensington, UK. [2]Institute of Neuroinformatics, University of Zürich/ETH Zürich, Zürich, Switzerland. [3]These authors contributed equally to this work. Correspondence should be addressed to N.P.F. (n.franks@imperial.ac.uk) or W.W. (w.wisden@imperial.ac.uk).

Received 26 November 2014; accepted 21 January 2015; published online 23 February 2015; doi:10.1038/nn.3957

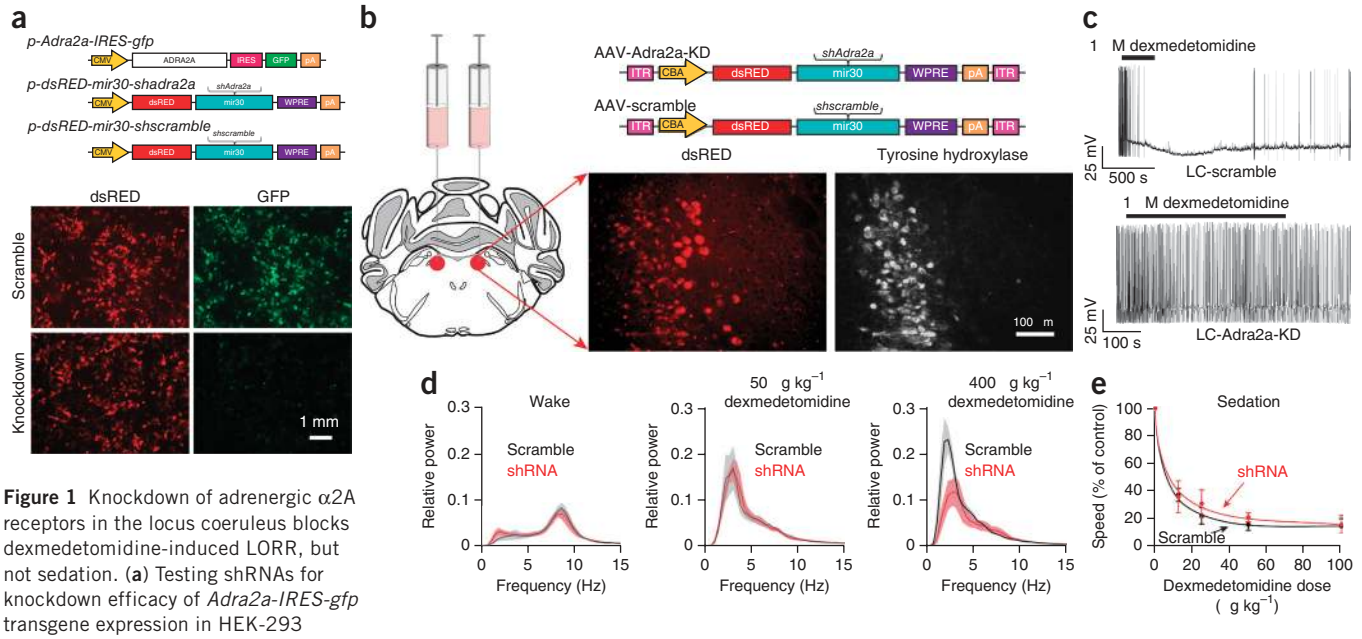

Figure 1 Knockdown of adrenergic α2A receptors in the locus coeruleus blocks dexmedetomidine-induced LORR, but not sedation. (**a**) Testing shRNAs for knockdown efficacy of *Adra2a-IRES-gfp* transgene expression in HEK-293 cells ($n = 8$). The photographs show transfected HEK-293 cells; GFP fluorescence (green) was strongly reduced with the *shAdra2a*$_1$ construct, but not with the scramble version. The dsRED expression revealed similar transfection efficiencies. CMV, cytomegalovirus promoter/enhancer region; IRES, internal ribosome entry site; pA, polyadenylation sequence; WPRE, woodchuck post-transcriptional regulatory element. (**b**) AAVs expressing either dsRED-mir30-shAdra2a or dsRED-mir30-shscramble were bilaterally injected into the LC of adult mice. Photographs illustrate transgene expression (dsRED) in the LC as confirmed by co-staining with tyrosine hydroxylase antisera (white). ITR, inverted terminal repeats; CBA, chicken-β-actin enhancer/promoter. (**c**) Whole-cell recordings of action potentials of LC neurons in acute slices from LC-scramble, and LC-Adra2a-KD mice. Applying dexmedetomidine to scramble-expressing neurons hyperpolarized the membrane potential and the neurons stopped firing; by contrast, dexmedetomidine had no effect on the neurons from the LC-Adra2a-KD mice ($P = 0.7$, $n = 7$ cells). (**d**) Fourier transform power spectra for LC-scramble (black) and LC-Adra2a-KD (red) mice in the waking state (left, $n = 5$) and in response to 50 μg kg^{-1} dexmedetomidine (middle, $n = 4$) and 400 μg kg^{-1} dexmedetomidine (right, $n = 4$). Lighter shaded envelopes indicate the s.e.m. (**e**) Movement of LC-scramble (black, $n = 4$–6), and LC-Adra2a-KD (red, $n = 4$–7) mice in response to sedative doses of dexmedetomidine were not significantly different (two-way ANOVA, $P = 0.91$). Error bars represent ±s.e.m.

determined how this affected sedation and LORR. We first selected two *Adra2a* shRNA sequences to use *in vivo*. For this, four putative *Adra2a* shRNA sequences (*shAdra2a*) were placed into a microRNA gene, *mir30* (ref. 28) (**Fig. 1a**). Two of the *Adra2a* hairpin sequences (*shAdra2a*$_1$ and *shAdra2a*$_2$) substantially reduced GFP expression from a reporter gene, *Adra2a-IRES-gfp*, coexpressed in HEK293 cells (**Fig. 1a**). The *dsRED-mir30-shAdra2a*$_1$, *dsRED-mir30-shAdra2a*$_2$ and *dsRED-mir30-shscramble* cassettes were then placed into adeno-associated virus (AAV) genomes, packaged and injected bilaterally into the LC (**Fig. 1b**). In the following section, similar results were obtained with both *shAdra2a* sequences; all *in vivo* results are illustrated for *shAdra2a*$_1$. The treated animals are termed LC-Adra2a-KD and LC-scramble. We obtained, on average, a knockdown to 46.3 ± 9.2% (mean ± s.e.) of control *Adra2a* transcript levels (*t* test, $P < 0.004$, compared with mRNA levels in the LC area of LC-scramble mice). We prepared acute slices from brainstem of LC-Adra2a-KD and LC-scramble mice and examined the electrophysiological responses of LC noradrenergic neurons to the α2 agonist dexmedetomidine (**Fig. 1c**). Dexmedetomidine (1 μM), when applied to LC-scramble neurons, inhibited action potential firing, hyperpolarizing the membrane potential by 9.8 ± 2 mV (mean ± s.e.m., $n = 6$ cells), as shown previously for other noradrenergic α2 agonists[9,10,29]. However, in LC-Adra2a-KD neurons, dexmedetomidine failed to block action potential firing (**Fig. 1c**) and the membrane potential did not change significantly ($P = 0.7$, $n = 7$ cells). Thus, the knockdown of *Adra2a* gene expression by approximately 50% removed the ability of dexmedetomidine to silence LC neurons. This is consistent with studies on heterozygote *Adra2a* global knockout mice, which found that the *Adra2a* allele shows strong haplo-insufficiency, whereby even at a high dose of dexmedetomidine (433 μg per kg of body weight), dexmedetomidine-induced LORR in *Adra2a* knockout mice was abolished[30].

We next injected a high dose of dexmedetomidine (400 μg per kg, intraperitoneal (i.p.)) into LC-scramble or LC-Adra2a-KD mice. All LC-scramble mice ($n = 9$) achieved LORR measured 10 min after dexmedetomidine injection; there was a concomitant large increase in delta power in the electroencephalogram (EEG; **Fig. 1d**). By contrast, only 25% of LC-Adra2a-KD mice achieved LORR following dexmedetomidine injection ($n = 8$, Fisher's exact test, $P = 0.0023$); there was still an increase in EEG delta power in these mice, but it was about half that of control (scramble injected) mice (**Fig. 1d**). Thus, we found that, in contrast with studies in mice with global dopamine-β-hydroxylase knockouts[16,17], but consistent with earlier proposals[11], α2A receptors on LC neurons were needed for α2 adrenergic agonist-induced LORR, and their knock-down caused a reduction in dexmedetomidine-induced delta power. We next gave a separate group of LC-Adra2a-KD and LC-scramble mice lower doses of dexmedetomidine (12.5–100 μg per kg). Both groups of mice showed equal ($P = 0.91$) sedation (**Fig. 1e**), becoming immobile and crouched, and with lowered heads. If prodded, they did respond briefly by walking, but then stopped. All sedated mice showed increases in EEG delta power ($n = 5$; **Fig. 1d**), whether or not the α2A receptor had been knocked down. Thus, α2A receptor expression on LC neurons was not necessary for α2 adrenergic receptor–induced sedation, a conclusion that surprised us, given that it was necessary for LORR. We reasoned that α2A agonist–induced LORR and sedation are distinct states, involving different neuronal groups.

© 2015 Nature America, Inc. All rights reserved.

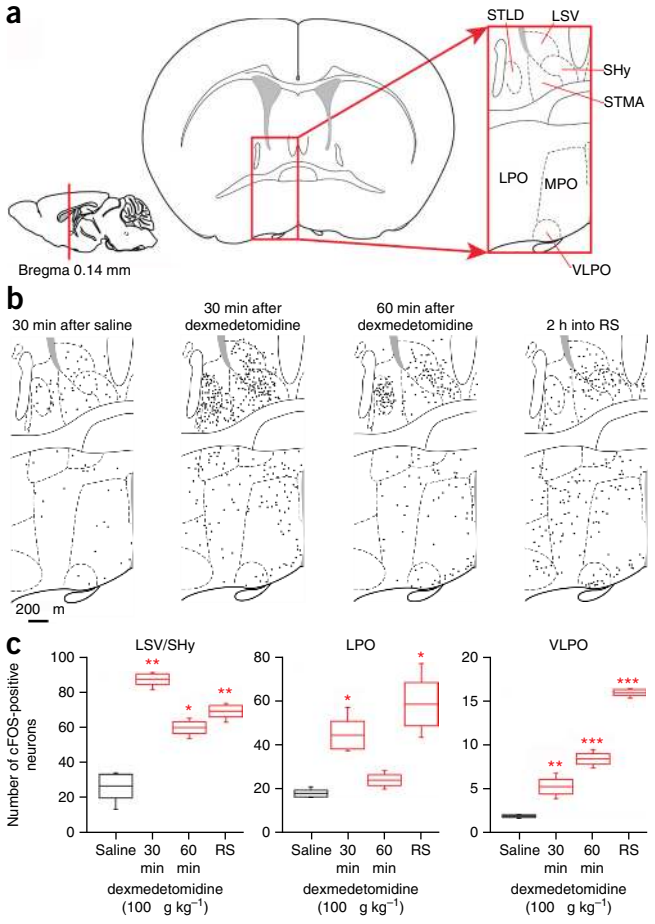

Figure 2 Dexmedetomidine-induced sedation and recovery sleep induced cFOS expression in overlapping regions of the mouse hypothalamic preoptic area and septum. (**a**) Schematic of the relevant preoptic hypothalamic and septal areas. Left, midline-sagittal section, red line marks position of the section. Middle, coronal section. Right, magnification of the boxed area showing the relevant anatomical sites. (**b**) Line drawings of cFOS protein expression in the boxed area at 30 min after saline injection and 30 or 60 min after dexmedetomidine (100 μg per kg) injections or 2 h into recovery sleep after sleep deprivation. Black dots represent cFOS-positive cells (see **Supplementary Fig. 1** for representative photographs). Relative to its expression after a saline injection, the endogenous *cFos* gene was induced widely in the area by sedative doses of dexmedetomidine or during recovery sleep. (**c**) Number of cFOS-positive neurons in selected anatomical sites after saline (white) or dexmedetomidine (red) injections or recovery sleep (gray). The boxes represent the s.e.m, and the bars show the range of the data. Asterisks represent significance relative to saline $*P < 0.05$, $**P < 0.01$, $***P < 0.001$ (*t* test).

TetTagging neurons in the preoptic hypothalamus

If not at the LC, where in the mouse brain does the α2 receptor–induced sedative response occur, and could natural sleep pathways be involved? Previous work emphasized that the ventrolateral preoptic (VLPO) nucleus in the PO hypothalamus was activated following dexmedetomidine administration[8] and during normal and recovery sleep[21,31], so we reviewed cFOS activation in the PO area. Mice were injected with a sedative dose of dexmedetomidine (100 μg per kg) or control saline. Brains were taken either 30 or 60 min afterwards and analyzed for endogenous cFOS expression (**Fig. 2** and **Supplementary Fig. 1**). We also investigated cFOS expression 2 h into the recovery sleep following 4 h of sleep deprivation (**Fig. 2** and **Supplementary Fig. 1**). Although for both dexmedetomidine-induced sedation and during recovery sleep there were some cFOS-positive neurons in VLPO, we found many more activated cells in the wider PO area (lateral preoptic area, LPO; medial preoptic area , MPO) and in a cluster of areas just dorsal of the preoptic region, in the BST (for example, in the stria terminalis medial anterior and stria terminalis lateral dorsal), and in several septal nuclei: the ventral lateral septum (LSV) and in the septo-hypothalamic nucleus (SHy) (**Fig. 2a–c**). Thus, the broadly similar patterns of induced cFOS during dexmedetomidine-induced sedation and during recovery sleep indicated that much of the PO region was a suitable location for TetTag-DREADD mapping[24–27] to see if activating neurons in this location was sufficient for to induce the behavioral states of sedation and recovery sleep. We aimed to express, by TetTagging[24], a *cFos*-promoter-inducible hM_3D_q-mCHERRY receptor gene[25,27] selectively in the PO area of the hypothalamus. The excitatory hM_3D_q metabotropic receptor is uniquely activated by the ligand CNO[27]. By combining this receptor with *cFos*-dependent TetTagging, the gene encoding the hM_3D_q receptor is only turned on following neural activity and so records, or tags, ensembles of neurons that have been activated *in vivo* by a stimulus[25]. The neurons can then be reactivated later by systemic CNO, allowing sufficiency for the particular behavior[25], sleep in this case, to be tested.

TetTagging has been developed with transgenic mice[24,25]. We set up the system using AAV genomes so that we could target the PO hypothalamus. Because of size constraints of the AAV genome, we generated two AAV viruses, one that contained the P_{cfos}-*tTA* transgene, and another that contained the *tet-operator* promoter ($P_{TRE\text{-}tight}$) linked to an hM_3D_q-*mCHERRY* receptor reading frame (**Fig. 3a**). With this method, before behavioral experiments are undertaken, the TetTag system is repressed with doxycycline in the diet. Doxycycline prevents tTA activating its target promoter, $P_{TRE\text{-}tight}$, located in the second AAV genome; when doxycycline is removed, neural activity, such as that occurring in recovery sleep or dexmedetomidine-induced sedation, can drive the *cFos* promoter–linked tTA expression, which in turn can activate hM_3D_q-*mCHERRY* expression (**Fig. 3a**).

Preliminary experiments revealed that, when AAV-P_{cfos}-tTA and AAV-$P_{TRE\text{-}tight}$-hM_3D_q-mCHERRY were co-injected, neurons were co-transduced. We therefore co-injected both the AAV-P_{cfos}-tTA and AAV-$P_{TRE\text{-}tight}$-hM_3D_q-mCHERRY bilaterally into LPO (LPO-TetTag-hM_3D_q mice) or centrally into the median PO, MnPO (MnPO-TetTag-hM_3D_q mice), the latter being an area in which neurons are particularly active in recovery sleep following sleep deprivation[19] (**Fig. 3b**). We maintained the mice for 4 weeks on a doxycycline diet. Doxycycline was then removed from the diet to allow potential inducibility of the hM_3D_q-mCHERRY gene, and mice were given either a sedative dose of dexmedetomidine (100 μg per kg) i.p., a control saline injection i.p. or 4 h of sleep deprivation 2 d later, and then allowed recovery sleep. In about half of the cohort, the dexmedetomidine injection and sleep deprivation procedures were switched (**Fig. 3b**). The order of these procedures made no difference to the results.

In the virally injected animals, we looked at activity-inducible hM_3D_q-mCHERRY patterns in the LPO and MnPO. We looked at TetTag gene expression in these areas before and after mice were given the sedative dose of dexmedetomidine (100 μg per kg) or sleep deprived and then killed during recovery sleep (**Fig. 3c** and **Supplementary Fig. 2**). LPO-TetTag-hM_3D_q and MnPO-TetTag-hM_3D_q brains were taken 2 h before, or 2 h after animals received dexmedetomidine or a control saline injection, or 2 h into recovery sleep. They were analyzed for mCHERRY expression. Before dexmedetomidine injection or sleep deprivation, but with no doxycycline

© 2015 Nature America, Inc. All rights reserved.

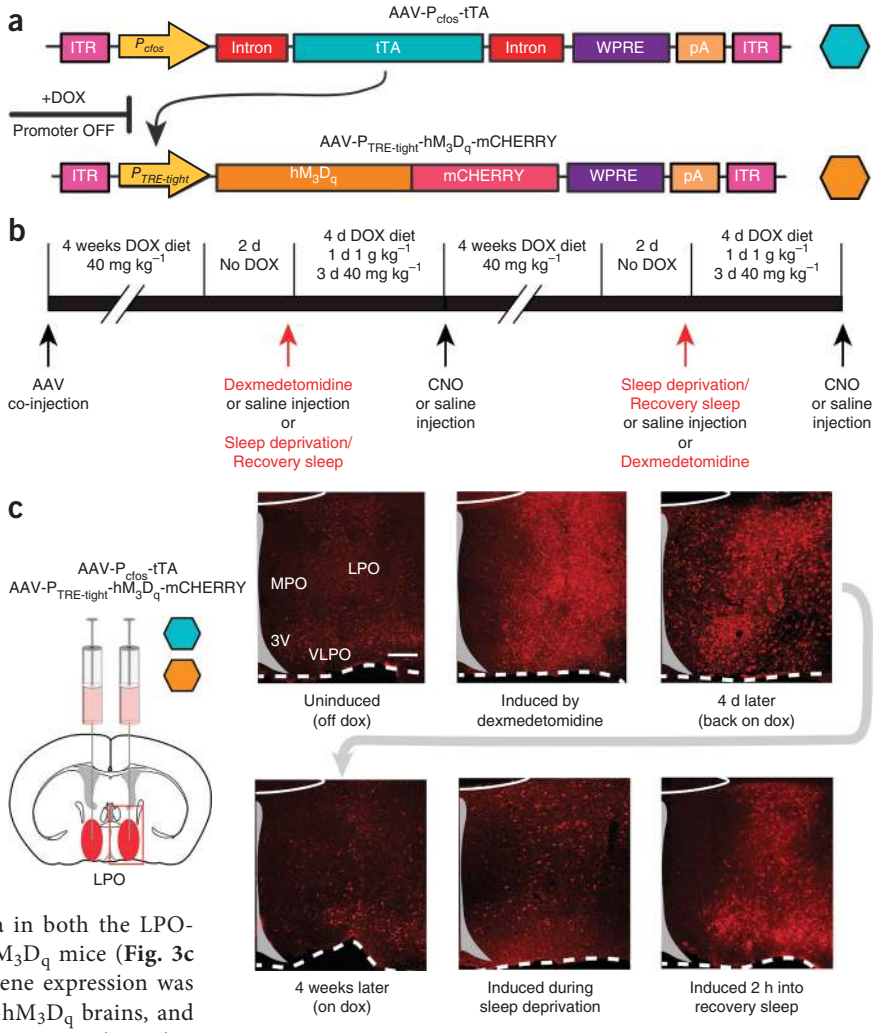

Figure 3 The TetTag-hM$_3$D$_q$ system to record and reactivate neuronal groups in the preoptic hypothalamus activated by a sedative dose of dexmedetomidine or during recovery sleep. (**a**) The AAV transgenes. The first contains the *cFos* promoter, which drives expression of tTA protein. In the presence of doxycycline (DOX), tTA cannot bind and activate its target promoter, $P_{TRE-tight}$, located in the second AAV genome. When doxycycline is removed, tTA can activate hM$_3$D$_q$-mCHERRY expression, but only in neurons in which tTA expression had been driven by the *cFos* promotor, reflecting neural activity. (**b**) The extended protocol and time line for the experiments. (**c**) LPO-TetTag-hM$_3$D$_q$ mice. Time course of $P_{TRE-tight}$-*hM$_3$D$_q$-mCHERRY* transgene induction and decay. The photographs show coronal sections from one side of the brain stained for hM$_3$D$_q$-mCHERRY expression (red), detected with mCHERRY antisera. The images were taken from animals killed at six time points: with doxycycline removed from the diet 2 d previously, just before dexmedetomidine-induced sedation; 2 h after a sedative dose of dexmedetomidine; 4 d later on and back on doxycycline, 4 weeks after dexmedetomidine-induced sedation on a doxycycline diet; 4 h after sleep deprivation; and 2 h into recovery sleep following sleep deprivation. Induced *hM$_3$D$_q$-mCHERRY* transgene expression was seen throughout the LPO area. Scale bar represents 200 μm.

present, there was a low, but detectable, level of P$_{TRE-tight}$-hM$_3$D$_q$-mCHERRY expression in scattered cells throughout the injected area in both the LPO-TetTag-hM$_3$D$_q$ mice and the MnPO-TetTag-hM$_3$D$_q$ mice (**Fig. 3c** and **Supplementary Fig. 2**). This basal transgene expression was also present with doxycycline. In LPO-TetTag-hM$_3$D$_q$ brains, and consistent with the induction of the endogenous *cFos* gene (**Fig. 2**), a wide area expressed hM$_3$D$_q$-mCHERRY receptors following systemic dexmedetomidine administration, stretching from the bed nucleus stria terminalis/lateral septum and septal hypothalamic nuclei in the dorsal part of the region, the whole LPO area and through to the VLPO and extended VLPO area at the base (**Fig. 3c**). For recovery sleep, a similar LPO-P$_{TRE-tight}$-hM$_3$D$_q$-mCHERRY expression pattern was found; this expression started to appear during the sleep deprivation period, and became stronger 2 h into recovery sleep (**Fig. 3c**). For the MnPO-TetTag-hM$_3$D$_q$ brains, recovery sleep and dexmedetomidine-induced sedation both induced hM$_3$D$_q$-mCHERRY expression above basal levels in the MnPO area; however, there was a differential effect, as the gene induction was weaker following dexmedetomidine-induced sedation compared with that during recovery sleep (**Supplementary Fig. 2**). In separate experiments, we determined that levels of the induced hM$_3$D$_q$-mCHERRY receptor protein persisted for at least 4 d post-stimulus (for example, dexmedetomidine-induced sedation or recovery sleep after sleep deprivation followed immediately by doxycycline in the diet; **Fig. 3c** and **Supplementary Fig. 2**), but that during the 4-week period following the first challenge, sleep-deprivation or dexmedetomidine-induced sedation, levels TetTag-hM$_3$D$_q$-mCHERRY expression fell back to baseline levels (**Fig. 3c** and **Supplementary Figs. 2–4**).

CNO induced the expression of *cFos* protein in TetTagged hM$_3$D$_q$-mCHERRY–positive neurons (**Supplementary Fig. 5**), suggesting that an excitatory response was generated in these neurons. To confirm this, we patch-clamped visually identified (mCHERRY positive) Tet-Tagged neurons found in acute PO slices after dexmedetomidine-induced sedation. In neurons that were TetTagged, we found that CNO induced an excitatory response (8 of 8 neurons in 3 animals) and was able to trigger action potential firing (**Supplementary Fig. 6a**). The average depolarization was 10.2 ± 2.1 mV in response to 5 μM CNO. As expected, these results are consistent with the hM$_3$D$_q$ receptor coupling to excitatory mechanisms[27]. After recording from the TetTagged neurons, we used single-cell quantitative PCR (qPCR) to determine their type: 84% were GABAergic (*Gad1* and/or *Gad2* expression) and the remaining were glutamatergic (*Vglut2* expression) (**Supplementary Fig. 6b,c**).

Recapitulation of recovery sleep and sedation by CNO

The following sequence of results is illustrated with LPO-TetTag-hM$_3$D$_q$ and MnPO-TetTag-hM$_3$D$_q$ mice first undergoing dexmedetomidine-induced sedation, followed by CNO treatment, then after a 1 month gap, 4-h sleep deprivation and recovery sleep followed by CNO treatment (**Figs. 4** and **5**). Approximately 5 min after dexmedetomidine injection, the EEG of both LPO-TetTag-hM$_3$D$_q$ and MnPO-TetTag-hM$_3$D$_q$ mice exhibited prominent and sustained NREM that lasted ~90 min relative to the mice given only saline (**Figs. 4a** and **5a**). All dexmedetomidine-injected mice became immobile (**Fig. 4b**), but still had a righting reflex. We put mice back on the doxycycline diet for 4 d to repress the induction of further

© 2015 Nature America, Inc. All rights reserved.

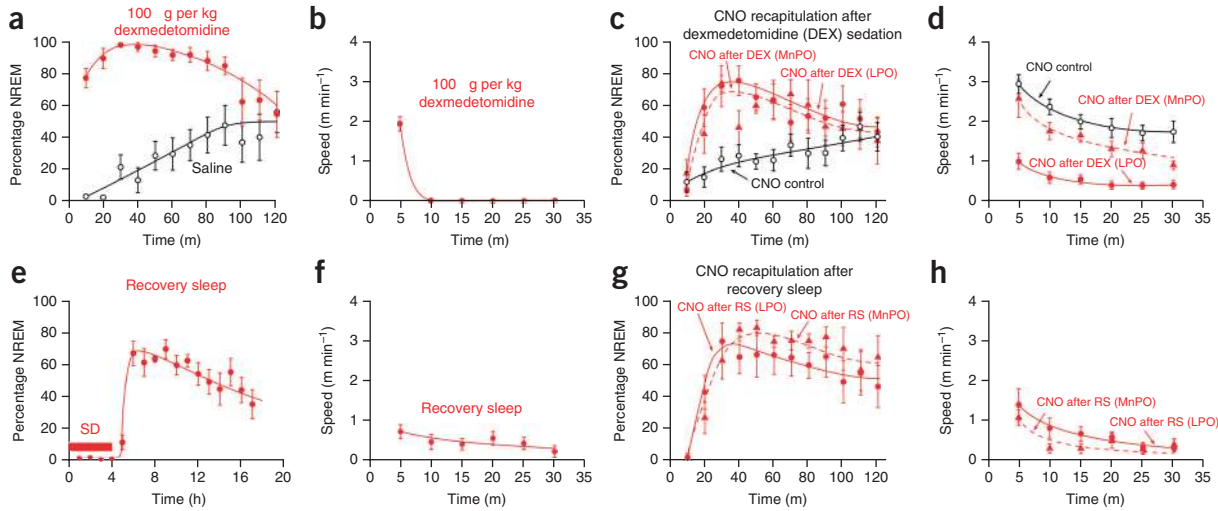

Figure 4 Serial re-activation of genetically tagged neuronal ensembles following dexmedetomidine-induced sedation and recovery sleep. (**a**) Percentage NREM sleep after dexmedetomidine. Both LPO-TetTag-hM$_3$D$_q$ ($n = 6$) and MnPO-TetTag-hM$_3$D$_q$ ($n = 6$) mice showed sustained NREM, significantly greater than control ($P < 0.0001$). Data shown are for LPO-TetTag-hM$_3$D$_q$ mice. (**b**) Speed in an open field 30 min after dexmedetomidine. Data shown are for LPO-TetTag-hM$_3$D$_q$ mice ($n = 7$). (**c**) NREM sleep after CNO injection, 4 d after dexmedetomidine sedation. Filled circles indicate LPO-TetTag-hM$_3$D$_q$ mice ($n = 7$, $P < 0.0001$, compared with control) after CNO injection. Filled triangles represent MnPO-TetTag-hM$_3$D$_q$ ($n = 6$, $P < 0.001$, compared with control) mice after CNO injection. Open circles indicate LPO-TetTag-hM$_3$D$_q$ ($n = 9$) mice after control CNO injection without prior sedation or recovery sleep. (**d**) Speed in an open field 30 min after CNO injection, 4 d after dexmedetomidine sedation. Filled circles represent after CNO injection for LPO-TetTag-hM$_3$D$_q$ mice. Filled triangles represent after CNO injection for MnPO-TetTag-hM$_3$D$_q$ mice. Open circles represent after control CNO injection without prior sedation or recovery sleep. CNO recapitulated the effects of dexmedetomidine in LPO-TetTag-hM$_3$D$_q$ ($n = 8$, $P < 0.0001$), but not in MnPO-TetTag-hM$_3$D$_q$ mice ($n = 6$, $P = 0.1$) compared with control ($n = 7$). (**e**) NREM after 4 h of sleep deprivation (SD, $n = 6$). (**f**) Speed in an open field 30 min at the start of recovery sleep ($n = 8$). (**g**) NREM sleep after CNO injection, 4 d after sleep deprivation/recovery sleep. Filled circles represent LPO-TetTag-hM$_3$D$_q$ mice ($n = 8$, $P < 0.0001$, compared to baseline) after CNO injection. Filled triangles represent MnPO-TetTag-hM$_3$D$_q$ ($n = 7$, $P < 0.0001$, two-way ANOVA compared to baseline) mice after CNO injection. (**h**) Speed in open field 30 min after CNO injection, 4 d after recovery sleep. CNO recapitulated the effects of recovery sleep in both LPO-TetTag-hM$_3$D$_q$ ($n = 8$; $P < 0.0001$) and in MnPO-TetTag-hM$_3$D$_q$ mice ($n = 7$; $P < 0.0001$, two-way ANOVA) compared to baseline ($n = 7$). For all panels, error bars represent s.e.m. and the statistical tests were two-way ANOVA.

© 2015 Nature America, Inc. All rights reserved.

npg

TetTag-hM$_3$D$_q$ receptors, injected them i.p. with CNO or saline and then recorded their EEG and behavioral responses (**Figs. 4c**,**d** and **5b**). The mice used in our study exhibited maximal periods of NREM sleep during the 'lights on' part of the cycle (**Supplementary Fig. 7a**,**b**). All CNO injections were therefore carried out during this period when the mice were most active.

After CNO injection, the LPO-TetTag-hM$_3$D$_q$ mice went into a state resembling sustained NREM sleep (**Figs. 4c**,**d** and **5b**). They moved little and their neocortical EEG developed powerful and sustained delta activity for about 90 min. Thus, dexmedetomidine-induced sedation was recapitulated by CNO injection.

Giving CNO to the MnPO-TetTag-hM$_3$D$_q$ mice that were previously sedated with dexmedetomidine induced substantial delta power (high delta/theta ratio) in the EEG (**Figs. 4c** and **5c**), but these mice moved to a similar extent as the saline- or CNO-injected controls (**Fig. 4d**). Thus, there was a notable disconnect between EEG and behavior. This suggests that the LPO area, but not the MnPO, contains neurons sufficient for full adrenergic α2 receptor–induced sedation.

Prior to the next stimulus, sleep deprivation followed by recovery sleep, LPO-TetTag-hM$_3$D$_q$ and MnPO-TetTag-hM$_3$D$_q$ mice were maintained on doxycycline for a further 4 weeks. CNO administration to these animals during the latter part of this time had no effect on the behavior or EEG, consistent with the decay of the hM$_3$D$_q$-mCHERRY protein back to basal levels (**Fig. 3c** and **Supplementary Fig. 2**). About a month after the first experiment (dexmedetomidine-induced sedation), the mice were removed from doxycycline and, 48 h later, instead of a sedative dexmedetomidine injection, the mice were sleep deprived and then allowed a period of recovery sleep (**Fig. 4e**). During the recovery sleep, the EEG of both LPO-TetTag-hM$_3$D$_q$ and MnPO-TetTag-hM$_3$D$_q$ mice showed sustained NREM sleep (**Figs. 4e** and **5d**). During a 30-min recording, mice in recovery sleep moved little (**Fig. 4f**). After the period of sleep deprivation, the mice were placed back on doxycycline and, 4 d later, given a CNO or saline injection i.p. and their behavior and EEG responses were measured.

Both groups of CNO-injected mice, LPO-TetTag-hM$_3$D$_q$ and MnPO-TetTag-hM$_3$D$_q$ mice, had sustained delta power ~90 min following CNO administration (**Figs. 4g** and **5e**,**f**), and strong behavioral arrest (**Fig. 4h**), showing that an ensemble of neurons had been activated in these areas that were sufficient to initiate and sustain recovery sleep. Given that these were the same group of animals that had earlier undergone dexmedetomidine-induced sedation and reactivation by CNO, it seems likely that dexmedetomidine-induced sedation and recovery sleep share similar mechanisms and circuitry for the LPO area. On the other hand, although MnPO seemed relevant for recovery sleep, where its re-activation seemed to be as effective as LPO's, MnPO had less of a role in dexmedetomidine-induced sedation.

Recapitulation of hypothermia by CNO

Using TetTagging, we examined whether the neural circuitries in the LPO and MnPO areas were sufficient to trigger sedative or recovery sleep–induced hypothermia. Before any treatments, we checked that neither saline nor CNO injections caused a change in body temperature (**Fig. 6a**). The body temperature of the mice was higher during the dark period when they were most active (**Supplementary Fig. 7c**); as for the sedation experiments, all investigations of temperature were done during the dark period. 2 d after doxycycline removal, we gave LPO-TetTag-hM$_3$D$_q$ and MnPO-TetTag-hM$_3$D$_q$ mice the sedative dose of 100 μg per kg dexmedetomidine. This caused a strong

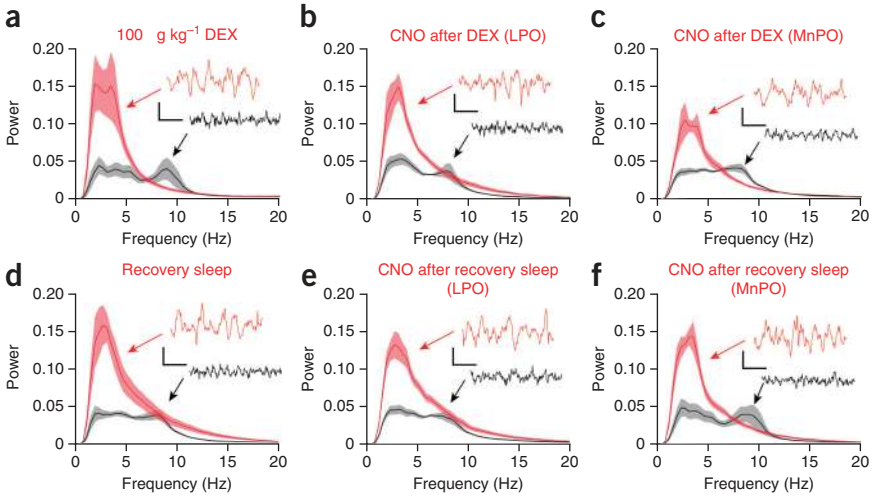

Figure 5 EEG delta power is recapitulated by reactivation of genetically tagged neuronal ensembles in LPO-TetTag-hM$_3$D$_q$ and MnPO-TetTag-hM$_3$D$_q$ mice following dexmedetomidine-induced sedation or recovery sleep. Each panel shows Fourier Transform power spectra when the EEG and electromyogram (EMG) signals were scored as either sleep (red) or wake (black). The envelopes represent the s.e.m. (**a**) Dexmedetomidine sedation ($n = 7$). (**b**) CNO reactivation after dexmedetomidine sedation for LPO-TetTag-hM$_3$D$_q$ mice ($n = 8$). (**c**) CNO reactivation after dexmedetomidine sedation for MnPO-TetTag-hM$_3$D$_q$ mice ($n = 6$). (**d**) Recovery sleep ($n = 7$). (**e**) CNO reactivation after recovery sleep for LPO-TetTag-hM$_3$D$_q$ mice ($n = 8$). (**f**) CNO reactivation after recovery sleep for MnPO-TetTag-hM$_3$D$_q$ mice ($n = 7$). Each spectrum is calculated by combining EEG segments totaling 20 min. The insets show representative EEG traces, and the accompanying calibration bars represent 100 μV and 500 ms.

hypothermia (**Fig. 6a**), consistent with previous reports[6,32]. 4 d later, on a doxycycline diet, we then injected them with CNO. In the LPO-TetTag-hM$_3$D$_q$ animals, CNO reactivation of the dexmedetomidine-induced hypothalamic ensembles largely recapitulated the temperature drop (**Fig. 6b**). There was, however, little effect in MnPO-TetTag-hM$_3$D$_q$ mice (**Fig. 6c**). Thus, following dexmedetomidine sedation, activated neuronal ensembles in LPO, but not MnPO, are responsible for the hypothermia produced by this drug.

A parallel group of LPO-TetTag-hM$_3$D$_q$ and MnPO-TetTag-hM$_3$D$_q$ mice were sleep deprived for 4 h and allowed recovery sleep. Sleep deprivation elevated their body temperature to about 38 °C; during the first few hours of recovery sleep, this temperature fell to that occurring during natural NREM sleep, about 36.5 °C (**Fig. 6d** and **Supplementary Fig. 7c**). 4 d later, we gave mice CNO. In both the LPO- and MnPO-TetTag-hM$_3$D$_q$ groups, CNO treatment produced a substantial drop in body temperature (**Fig. 6e**,**f**), comparable to, but somewhat larger than, that seen during recovery sleep (**Fig. 6d**). Thus, as we found for the effects on delta power and immobility, both LPO and MnPO can contribute equal and parallel effects in producing hypothermia in recovery sleep.

Role of GABAergic neurons for the rapid onset of sedation

To test whether dexmedetomidine-induced sedation required GABAergic neurons in the LPO area, we deleted the vesicular GABA transporter (*Vgat*) gene by injecting AAV-Cre-2A-Venus bilaterally into the LPO of mice homozygous for a *loxP*-flanked *Vgat* gene[33], *Vgat*$^{lox/lox}$, to generate LPO-*ΔVgat* mice (**Fig. 7a**). Control *Vgat*$^{lox/lox}$ mice were injected with AAV-GFP to give LPO-GFP mice.

1 month later, when given sedative doses of dexmedetomidine (100 μg per kg), and some 5 min after injection, control LPO-GFP mice showed the expected large increase in delta power in their EEG compared with that produced by saline injection (**Fig. 7b**), they had sustained NREM lasting for ~90 min (**Fig. 7c**), and in about 10 min after injection they had ceased moving (**Fig. 7d**). By contrast, 10 min after i.p. injection of dexmedetomidine into LPO-*ΔVgat* mice, there was only a small shift of the EEG to delta frequencies (**Fig. 7e**). This absence of effect was notable (**Fig. 7b**,**e**). However, ~30 min after injection, the percentage of NREM in the LPO-*ΔVgat* mice was substantially higher than in saline-injected animals (**Fig. 7f**), and the mice became sedated (**Fig. 7g**), such that after 30 min they were as sedated as dexmedetomidine-injected LPO-GFP mice (**Fig. 7c**,**f**). Thus, GABAergic neurons in the LPO area were required for rapid-onset dexmedetomidine-induced sedation.

Controls for the TetTag-DREADD method

We did several controls for the specificity of the TetTag-DREADD system. First, CNO given alone to mice that had not received any AAV injections produced no behavioral effects, no change to the EEG

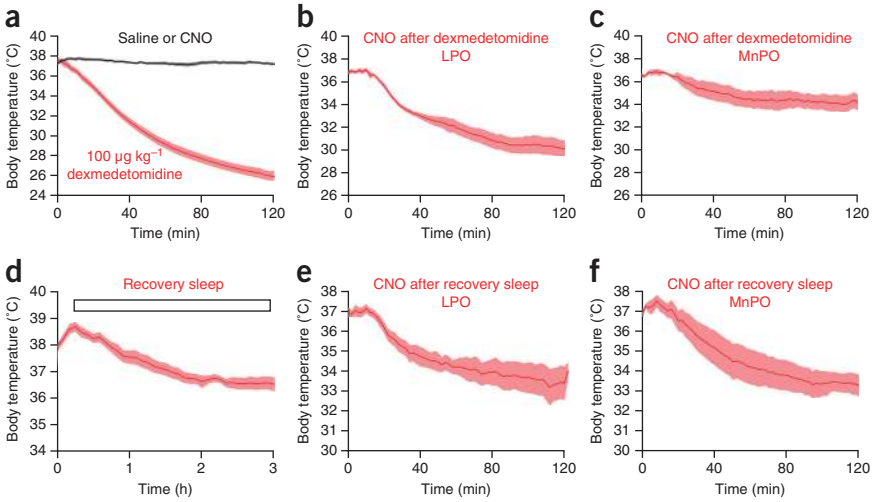

Figure 6 Hypothermia is recapitulated by reactivation of genetically tagged neuronal ensembles in LPO-TetTag-hM$_3$D$_q$ and MnPO-TetTag-hM$_3$D$_q$ mice following recovery sleep, but only in LPO-TetTag-hM$_3$D$_q$ mice following dexmedetomidine-induced sedation. (**a**–**f**) Changes in body temperature following dexmedetomidine sedation ($n = 10$, red) or saline ($n = 20$) or CNO ($n = 3$) (black) (**a**), CNO reactivation after dexmedetomidine sedation for LPO-TetTag-hM$_3$D$_q$ mice ($n = 5$, **b**), CNO reactivation after dexmedetomidine sedation for MnPO-TetTag-hM$_3$D$_q$ mice ($n = 5$, **d**), recovery sleep ($n = 10$, **d**), CNO reactivation after recovery sleep for LPO-TetTag-hM$_3$D$_q$ mice ($n = 6$, **e**), and CNO reactivation after recovery sleep for MnPO-TetTag-hM$_3$D$_q$ mice ($n = 5$, **f**). The data in **a** and **d** are for LPO-TetTag-hM$_3$D$_q$ and MnPO-TetTag-hM$_3$D$_q$ mice combined, as these were indistinguishable. The envelopes represent the s.e.m.

© 2015 Nature America, Inc. All rights reserved.

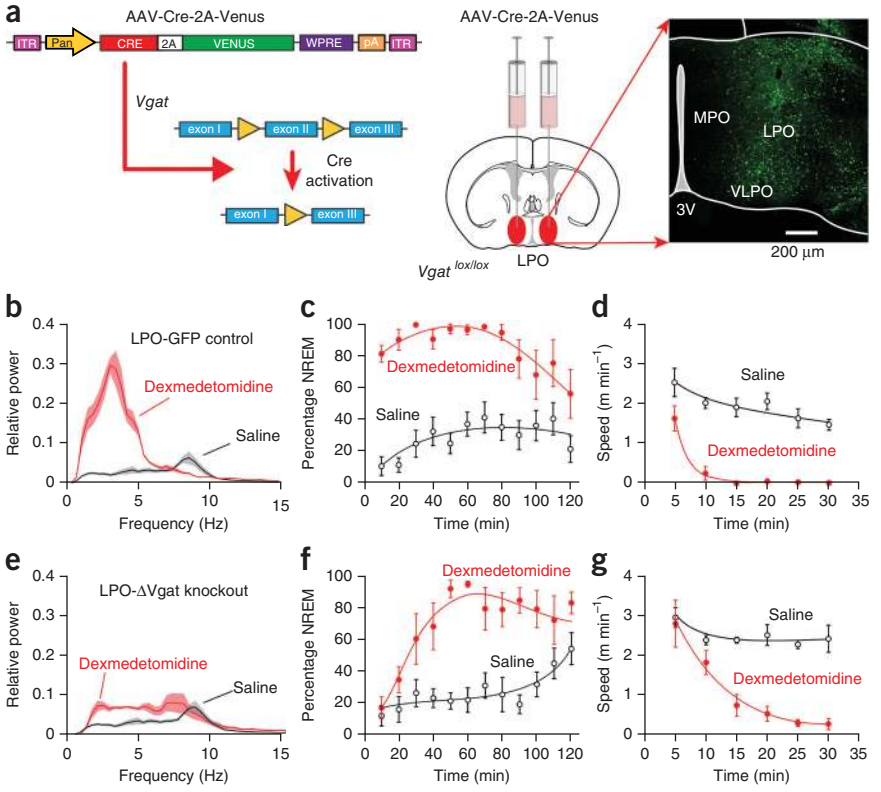

Figure 7 Selective knockout of the GABA vesicular transporter gene (*Vgat*) in the PO hypothalamic area (LPO-Δ*Vgat* mice) slows the transition to dexmedetomidine-induced sleep. (**a**) Cre recombinase, produced from an AAV transgene, deletes exon 2 of the *Vgat* gene[33] following AAV-Cre-2A-Venus bilateral injection into the LPO area of $Vgat^{lox/lox}$ mice. Right, the extent of AAV expression, as detected by staining with EGFP antisera. (**b**) EEG power spectra 10 min after dexmedetomidine (100 µg kg^{-1}, red line) or saline (black) injection in control mice ($n = 8$) expressing AAV-GFP in the LPO (LPO-GFP mice, $n = 6$). Lighter shaded envelopes indicate the s.e.m. (**c**) Percentage of time scored as NREM sleep after dexmedetomidine (100 µg per kg; filled circles, $n = 6$) was significantly greater (two-way ANOVA, $P < 0.0001$) than in saline (open circles, $n = 8$) in LPO-GFP control mice. (**d**) Speed in open field 30 min after dexmedetomidine (100 µg kg^{-1}, filled circles, $n = 7$) was significantly less (two-way ANOVA, $P < 0.0001$) than in saline (open circles, $n = 6$) in LPO-GFP control mice. (**e**) EEG power spectra 10 min after dexmedetomidine (100 µg per kg, red line, $n = 6$) or saline (black) injection in mice ($n = 8$) expressing AAV-Cre-2A-Venus in the LPO (LPO-ΔVgat mice). (**f**) Percentage of time scored as NREM sleep after dexmedetomidine (100 µg kg^{-1}, filled circles, $n = 6$) was significantly greater (two-way ANOVA, $P < 0.0001$) than in saline ($n = 8$) in AAV-Cre-2A-Venus mice. (**g**) Speed in open field 30 min after dexmedetomidine (100 µg kg^{-1}; filled circles, $n = 6$) was significantly less (two-way ANOVA, $P < 0.0001$) than in saline (open circles, $n = 8$) in LPO-ΔVgat mice. For all panels, the error bars represent s.e.m.

© 2015 Nature America, Inc. All rights reserved.

(as noted previously[27]) and no change in body temperature. Second, we found a low basal expression of the $P_{TRE\text{-}tight}$-hM_3D_q transgene in the PO hypothalamic area of AAV-injected mice on doxycycline (**Fig. 3c**). But even when we unlocked the transgene system by removing doxycycline for 2 d from the diet, and then giving CNO without any other treatments, nothing happened to the mice (**Fig. 4c**,**d**,**g**,**h**). Evidently, strong stimulation of the relevant neurons is needed to induce the TetTag genes. Third, we co-injected the AAV-P_{cfos}-tTA and AAV-$P_{TRE\text{-}tight}$-hM_3D_q-mCHERRY viruses bilaterally into the superior colliculi (**Supplementary Fig. 8a**), a region that is unlikely to be involved in either dexmedetomidine-induced sedation or recovery sleep after sleep deprivation.

These SC-TetTag-hM_3D_q mice were then subjected to the full experimental procedure (**Fig. 3b**): doxycycline repression for 1 month, doxycycline removal, dexmedetomidine-sedation followed by 4 d recovery and then CNO injection, and then, subsequently, the sleep deprivation and recovery sleep treatments, followed by CNO administration. No behavioral or EEG change was found (**Supplementary Fig. 8b**) and there was little basal or induced hM_3D_q-mCHERRY expression seen in the colliculi, suggesting that the sleep-recapitulating effect of CNO is specific for the PO hypothalamus.

DISCUSSION

Selectively activating α2-adrenoreceptors is an effective way to induce deep, but arousable, sedation[7,9,10,34]. The sleep-like qualities of this sedation hint that, by understanding how adrenergic α2 agonists work at the network level, we might learn more about circuitry regulating aspects of natural sleep. Global gene knockouts show that dexmedetomidine-induced sedation, hypothermia and LORR all depend on α2A receptors[9,32]. Given that α2A receptor activation inhibits noradrenergic LC neurons[9] (**Fig. 1c**) and LC firing promotes wakefulness[13–15], the view has been that α2-adrenergic agonists produce sedation by inhibiting the LC[7]. In many studies, sedation and LORR tend to be conceptually blended: sedation is considered a light or intermittent loss of consciousness, whereas LORR is a deeper version of this same state. We investigated this by acute knockdown of α2A receptors selectively from the LC. To our surprise, this did not alter dexmedetomidine's ability to induce sedation at low doses (<100 µg per kg), but did, on the other hand, abolish LORR at high concentrations (400 µg per kg). This suggests that these states, sedation and LORR, are generated by α2 agonist drugs influencing distinct circuitries; in particular, sedation induced by low-dose dexmedetomidine does not depend on inhibiting the LC.

We suggest that dexmedetomidine-induced LORR is not, in fact, the animal equivalent of deep loss of consciousness in humans, as usually assumed, but instead results from engaging the spinal cord mechanism that produces muscle atonia in REM sleep and cataplexy[35]. During wakefulness, GABAergic and glycinergic interneurons in the spinal cord and brainstem are inhibited by descending LC inputs[35]; this descending inhibition is released during REM sleep to give muscle atonia[35]. Thus, over-stimulating the noradrenergic LC neurons optogenetically, probably silencing them by vesicle depletion, causes a cataplexy-like state with muscle atonia[15]. Similarly, we speculate that high-dose dexmedetomidine causes LORR by inhibiting LC neurons, which in turn releases interneuron inhibition of motor neurons.

Dexmedetomidine sedation and recovery sleep are similar

In humans, the clinical use for dexmedetomidine is at the lower sedative doses. Thus, it is particularly important to understand the mechanism of this sedative component. A classic body of work shows

that the PO hypothalamic area regulates wakefulness, sleep and body temperature[18,23,36,37]. Sleep-active and temperature-sensitive neurons are widespread in the PO area[18–20]. Indeed, we found that an extensive part of the PO hypothalamus and some neighboring dorsal structures express both endogenous cFOS and the *cFos*-dependent *hM$_3$D$_q$-mCHERRY* transgene during recovery sleep and after dexmedetomidine-induced sedation. It was not clear, however, if activating any of these neurons is sufficient to induce sleep or the accompanying decrease in body temperature found with these states. To test their sufficiency, we reactivated the induced TetTag ensembles with systemic CNO.

By artificially reactivating the neurons initially activated by a systemic low-dose of dexmedetomidine, we found that such LPO neurons are sufficient to induce both sedation (NREM sleep) and the accompanying strong hypothermia. The rapid induction of this sedation required GABAergic neurons in the LPO area, but full sedation could still emerge later when GABA release was blocked, implying additional mechanisms. Because some of these neurons release galanin[38], this neuropeptide may also be involved. We also found that reactivating the same or similar groups of neurons in the LPO also mimicked recovery sleep and the drop in body temperature after sleep deprivation. Thus, TetTagging revealed that dexmedetomidine-induced sedation and recovery sleep are similar states, both requiring activation of neuronal ensembles in the LPO area. In the future, it will be interesting to disentangle the effects of sleep onset and body temperature decrease. Dexmedetomidine and sleep deprivation also induced TetTag-hM$_3$D$_q$ expression in another PO nucleus, MnPO. Although reactivation of MnPO with CNO did fully recapitulate recovery sleep, it only partially recapitulated DEX-induced sedation. There was an interesting disconnect between a strong increase in the EEG delta/theta ratio and animal movement—the mice were not sleeping, but perhaps 'sleep walking'. This was also true with the hypothermia effects: although MnPO could recapitulate the temperature decrease seen in recovery sleep, no ensembles that regulate temperature were activated in MnPO by dexmedetomidine sedation.

The natural sleep rhythm over 24 h was not a sufficiently strong stimulus to induce the TetTag-DREADD neuronal ensembles, at least under our experimental protocol: their formation apparently required the stronger drivers of dexmedetomidine or recovery sleep following sleep deprivation. In basal conditions, CNO did not induce a change in the EEG compared with dexmedetomidine sedation and recovery sleep, and animals did not behaviorally enter sleep. Indeed, in mice with hM$_3$D$_q$ receptors selectively, but continuously, expressed in GABAergic neurons in the PO hypothalamic area[39], systemic CNO produced only a small increase in NREM sleep, and only during the day.

A dominant hypothesis has been that NA tonically inhibits sleep-active GABAergic neurons in the PO area during wakefulness that project to arousal nuclei[40,41]. However, the TetTag method demonstrated that both α2 agonists and sleep deprivation induced NREM sleep and decreases in body temperature by locally exciting neurons in the preoptic area. One explanation for our results could be that adrenergic α2 agonists preferentially inhibit local GABAergic interneurons. These would in turn inhibit sleep-active GABAergic projection neurons less. Thus, following dexmedetomidine administration, the projection neurons would then fire more by dis-inhibition to induce sedation. However, a knockdown of *Adra2a* transcripts in the LPO did not alter the sedative effects of 100 μg per kg dexmedetomidine (**Supplementary Fig. 9**). Alternatively, dexmedetomidine could activate inhibitory α2A receptors on the terminals of inhibitory afferents coming into the PO area, for example, GABA inputs, or NA inputs from nuclei other than the LC. The reduced local release of GABA or NA into the PO hypothalamus would then allow dis-inhibition and excitation of the sleep-promoting neurons.

The biochemical mechanism for how recovery sleep is initiated and maintained remains a mystery. Candidate sleep homeostat molecules, which accumulate proportionally to the amount of sleep deprivation and act locally in the preoptic area, include PGD2 and adenosine[42]. Because hypothalamic-initiated recovery sleep and dexmedetomidine-induced sedation seem similar, another endogenous, but as yet unidentified, candidate sleep homeostat molecule might resemble an adrenergic α2 agonist in its properties.

METHODS

Methods and any associated references are available in the online version of the paper.

Note: Any Supplementary Information and Source Data files are available in the online version of the paper.

ACKNOWLEDGMENTS

This work was supported by the Medical Research Council (G0901892, N.P.F., S.G.B. and W.W.; G0800399, W.W.), the Biotechnology and Biological Sciences Research Council (BBSRC) (G021691 and BB/K018159/1, N.P.F., S.G.B. and W.W.), the Wellcome Trust (WT094211MA, S.G.B., N.P.F. and W.W.), a BBSRC CASE studentship (E.A.S.), a Wellcome Trust Vacation Scholarship (Z.E.P.), a BBSRC doctoral training grant (BB/F017324/1, E.C.H.), UK-China Scholarships for Excellence/China Scholarship scheme (X.Y. and Z.Y.) and the ERASMUS program (İ.G. and A.M.).

AUTHOR CONTRIBUTIONS

N.P.F. and W.W. conceived and designed the experiments. Z.Z., V.F., İ.G., A.M., E.A.S., Z.Y., A.Y.Z., X.Y., R.Y., Z.E.P. and E.C.H. performed the experiments. A.L.V. provided the Neurologgers. N.P.F., W.W. and S.G.B. contributed to the data analysis. N.P.F. and W.W. wrote the paper.

COMPETING FINANCIAL INTERESTS

The authors declare no competing financial interests.

Reprints and permissions information is available online at http://www.nature.com/reprints/index.html.

1. Franks, N.P. General anaesthesia: from molecular targets to neuronal pathways of sleep and arousal. *Nat. Rev. Neurosci.* **9**, 370–386 (2008).
2. Rihel, J. & Schier, A.F. Sites of action of sleep and wake drugs: insights from model organisms. *Curr. Opin. Neurobiol.* **23**, 831–840 (2013).
3. Adams, R. *et al.* Efficacy of dexmedetomidine compared with midazolam for sedation in adult intensive care patients: a systematic review. *Br. J. Anaesth.* **111**, 703–710 (2013).
4. Bol, C.J.J.G., Danhof, M., Stanski, D.R. & Mandema, J.W. Pharmacokinetic-pharmacodynamic characterization of the cardiovascular, hypnotic, EEG and ventilatory responses to dexmedetomidine in the rat. *J. Pharmacol. Exp. Ther.* **283**, 1051–1058 (1997).
5. Seidel, W.F., Maze, M., Dement, W.C. & Edgar, D.M. Alpha-2 adrenergic modulation of sleep: time-of-day-dependent pharmacodynamic profiles of dexmedetomidine and clonidine in the rat. *J. Pharmacol. Exp. Ther.* **275**, 263–273 (1995).
6. MacDonald, E., Scheinin, M., Scheinin, H. & Virtanen, R. Comparison of the behavioral and neurochemical effects of the two optical enantiomers of medetomidine, a selective alpha-2-adrenoceptor agonist. *J. Pharmacol. Exp. Ther.* **259**, 848–854 (1991).
7. Sanders, R.D. & Maze, M. Noradrenergic trespass in anesthetic and sedative states. *Anesthesiology* **117**, 945–947 (2012).
8. Nelson, L.E. *et al.* The alpha2-adrenoceptor agonist dexmedetomidine converges on an endogenous sleep-promoting pathway to exert its sedative effects. *Anesthesiology* **98**, 428–436 (2003).
9. Lakhlani, P.P. *et al.* Substitution of a mutant alpha2a-adrenergic receptor via "hit and run" gene targeting reveals the role of this subtype in sedative, analgesic, and anesthetic-sparing responses *in vivo*. *Proc. Natl. Acad. Sci. USA* **94**, 9950–9955 (1997).
10. Aghajanian, G.K. & VanderMaelen, C.P. α_2-adrenoceptor-mediated hyperpolarization of locus coeruleus neurons: intracellular studies *in vivo*. *Science* **215**, 1394–1396 (1982).
11. Correa-Sales, C., Rabin, B.C. & Maze, M. A hypnotic response to dexmedetomidine, an alpha 2 agonist, is mediated in the locus coeruleus in rats. *Anesthesiology* **76**, 948–952 (1992).
12. Takahashi, K., Kayama, Y., Lin, J.S. & Sakai, K. Locus coeruleus neuronal activity during the sleep-waking cycle in mice. *Neuroscience* **169**, 1115–1126 (2010).

© 2015 Nature America, Inc. All rights reserved.

13. Berridge, C.W., Schmeichel, B.E. & Espana, R.A. Noradrenergic modulation of wakefulness/arousal. *Sleep Med. Rev.* **16**, 187–197 (2012).
14. Carter, M.E., de Lecea, L. & Adamantidis, A. Functional wiring of hypocretin and LC-NE neurons: implications for arousal. *Front. Behav. Neurosci.* **7**, 43 (2013).
15. Carter, M.E. *et al.* Tuning arousal with optogenetic modulation of locus coeruleus neurons. *Nat. Neurosci.* **13**, 1526–1533 (2010).
16. Gilsbach, R. *et al.* Genetic dissection of alpha2-adrenoceptor functions in adrenergic versus nonadrenergic cells. *Mol. Pharmacol.* **75**, 1160–1170 (2009).
17. Hu, F.Y. *et al.* Hypnotic hypersensitivity to volatile anesthetics and dexmedetomidine in dopamine beta-hydroxylase knockout mice. *Anesthesiology* **117**, 1006–1017 (2012).
18. Szymusiak, R., Gvilia, I. & McGinty, D. Hypothalamic control of sleep. *Sleep Med.* **8**, 291–301 (2007).
19. Alam, M.A., Kumar, S., McGinty, D., Alam, M.N. & Szymusiak, R. Neuronal activity in the preoptic hypothalamus during sleep deprivation and recovery sleep. *J. Neurophysiol.* **111**, 287–299 (2014).
20. Takahashi, K., Lin, J.S. & Sakai, K. Characterization and mapping of sleep-waking specific neurons in the basal forebrain and preoptic hypothalamus in mice. *Neuroscience* **161**, 269–292 (2009).
21. Sherin, J.E., Shiromani, P.J., McCarley, R.W. & Saper, C.B. Activation of ventrolateral preoptic neurons during sleep. *Science* **271**, 216–219 (1996).
22. Lu, J., Greco, M.A., Shiromani, P. & Saper, C.B. Effect of lesions of the ventrolateral preoptic nucleus on NREM and REM sleep. *J. Neurosci.* **20**, 3830–3842 (2000).
23. Saper, C.B., Fuller, P.M., Pedersen, N.P., Lu, J. & Scammell, T.E. Sleep state switching. *Neuron* **68**, 1023–1042 (2010).
24. Reijmers, L.G., Perkins, B.L., Matsuo, N. & Mayford, M. Localization of a stable neural correlate of associative memory. *Science* **317**, 1230–1233 (2007).
25. Garner, A.R. *et al.* Generation of a synthetic memory trace. *Science* **335**, 1513–1516 (2012).
26. Reijmers, L. & Mayford, M. Genetic control of active neural circuits. *Front. Mol. Neurosci.* **2**, 27 (2009).
27. Alexander, G.M. *et al.* Remote control of neuronal activity in transgenic mice expressing evolved G protein–coupled receptors. *Neuron* **63**, 27–39 (2009).
28. Stegmeier, F., Hu, G., Rickles, R.J., Hannon, G.J. & Elledge, S.J. A lentiviral microRNA-based system for single-copy polymerase II-regulated RNA interference in mammalian cells. *Proc. Natl. Acad. Sci. USA* **102**, 13212–13217 (2005).
29. Zecharia, A.Y. *et al.* The involvement of hypothalamic sleep pathways in general anesthesia: testing the hypothesis using the $GABA_A$ receptor beta3N265M knock-in mouse. *J. Neurosci.* **29**, 2177–2187 (2009).
30. Tan, C.M., Wilson, M.H., MacMillan, L.B., Kobilka, B.K. & Limbird, L.E. Heterozygous alpha 2A-adrenergic receptor mice unveil unique therapeutic benefits of partial agonists. *Proc. Natl. Acad. Sci. USA* **99**, 12471–12476 (2002).
31. Gong, H. *et al.* Activation of c-fos in GABAergic neurones in the preoptic area during sleep and in response to sleep deprivation. *J. Physiol.* (*Lond.*) **556**, 935–946 (2004).
32. Hunter, J.C. *et al.* Assessment of the role of alpha2-adrenoceptor subtypes in the antinociceptive, sedative and hypothermic action of dexmedetomidine in transgenic mice. *Br. J. Pharmacol.* **122**, 1339–1344 (1997).
33. Tong, Q., Ye, C.P., Jones, J.E., Elmquist, J.K. & Lowell, B.B. Synaptic release of GABA by AgRP neurons is required for normal regulation of energy balance. *Nat. Neurosci.* **11**, 998–1000 (2008).
34. Drew, G.M., Gower, A.J. & Marriott, A.S. Alpha 2-adrenoceptors mediate clonidine-induced sedation in the rat. *Br. J. Pharmacol.* **67**, 133–141 (1979).
35. McGregor, R. & Siegel, J.M. Illuminating the locus coeruleus: control of posture and arousal. *Nat. Neurosci.* **13**, 1448–1449 (2010).
36. McGinty, D.J. & Sterman, M.B. Sleep suppression after basal forebrain lesions in the cat. *Science* **160**, 1253–1255 (1968).
37. Sterman, M.B. & Clemente, C.D. Forebrain inhibitory mechanisms: sleep patterns induced by basal forebrain stimulation in the behaving cat. *Exp. Neurol.* **6**, 103–117 (1962).
38. Sherin, J.E., Elmquist, J.K., Torrealba, F. & Saper, C.B. Innervation of histaminergic tuberomammillary neurons by GABAergic and galaninergic neurons in the ventrolateral preoptic nucleus of the rat. *J. Neurosci.* **18**, 4705–4721 (1998).
39. Saito, Y.C. *et al.* GABAergic neurons in the preoptic area send direct inhibitory projections to orexin neurons. *Front. Neural Circuits* **7**, 192 (2013).
40. Gallopin, T. *et al.* Identification of sleep-promoting neurons *in vitro*. *Nature* **404**, 992–995 (2000).
41. Modirrousta, M., Mainville, L. & Jones, B.E. Gabaergic neurons with alpha2-adrenergic receptors in basal forebrain and preoptic area express c-Fos during sleep. *Neuroscience* **129**, 803–810 (2004).
42. Brown, R.E., Basheer, R., McKenna, J.T., Strecker, R.E. & McCarley, R.W. Control of sleep and wakefulness. *Physiol. Rev.* **92**, 1087–1187 (2012).

© 2015 Nature America, Inc. All rights reserved.

ONLINE METHODS

Design and testing of *Adra2a* shRNAs. The mouse *Adra2a* coding region, including the start and stop codons, was obtained by PCR from the single exon *adra2* gene in genomic DNA (primer sequences given in reference[43]) and cloned into an expression plasmid pP_{cmv}-*IRES-gfp* (Clontech) upstream of the *IRES* element, between *XhoI* and EcoRI sites, to give *p*P_{cmv}-*Adra2a-IRES-gfp* (**Fig. 1a**). We used the Invitrogen and pSM2 design (http://cancan.cshl.edu/RNAi_central/) algorithms to select shRNAs directed against the mouse *Adra2a* coding or 3′UTR regions. To express the shRNAs, we used the pPRIME system[28]. This generates micro-RNA-30 (mir30)-derived shRNAs and co-expression of a marker protein, such as dsRED, from the same transcript. The shRNA hairpin sequences were placed into the mir30 site of *pPRIME-cmv-dsRed-FF3* (ref. 28) (Addgene Plasmid 11664; gift from S. Elledge, Howard Hughes Medical Institute). The DNA sequences of the hairpins (21 nucleotides) were *shAdra2a1*: 5′-TGC TGT TGA CAG TGA GCG AGC AACG TGC TGG TTA TTA TCG TAG TGA AGC CAC AGA TGT ACG ATA ATA ACC AGC ACG TTG CCT GCC TAC TGC CTC GGA-3′; *shAdra2a2*: 5′-TGC TGT TGA CAG TGA GCG CGC CAC TCA TCT CCA TAG AGA ATA GTG AAG CCA CAG ATG TAT TCT CTA TGG AGA TGA GTG GCG TGC CTA CTG CCT CGG A-3′; and *shscramble*: 5′-TGC TGT TGA CAG TGA GCG AGC CGC GAT TAG GCT GTT ATA ATA GTG AAG CCA CAG ATG TAT TAT AAC AGC CTA ATC GCG CGG CTT GCC TAC TGC CTC GGA-3′.

The hairpin oligonucleotides were PCR amplified by VENT polymerase (NEB) using the pPRIME forward and reverse oligonucleotides with added *XhoI* and EcoRI sites underlined (forward: 5′-GATGGCTG-CTCGAG-AAGGTATAT-TGCTGTTGACAGTGAGCG-3′; reverse, 5′-GTCTAGAG-GAATTC-CGAGGCAGTAGGCA-3′), digested with *XhoI* and EcoRI, and inserted into the mir30 site of EcoRI/*XhoI*-digested pPRIME to generate the constructs shown in **Figure 1a**. To test knockdown efficiency of the *shadra2* hairpins, HEK293 cells European Collection of Cell Cultures were co-transfected, using the calcium phosphate method, with *p*P_{cmv}-*Adra2a-IRES-gfp* and the *pPRIME-dsRED-mir30* plasmids. 16 h after transfection, cells were washed with PBS, and 48 h afterwards, the coverslips were then fixed, and mounted.

Generation of AAV *shAdra2a1*, *shAdra2a2* KD and *shscramble* transgenes. To generate AAV transgene-expressing miRNAs, the *dsRED-mir30-shAdra2a1*, *dsRED-mir30-shAdra2a2*, and *dsRED-mir30-shscramble* inserts in pPRIME[28] were released by *SbfI* and *PacI* digestion, and cloned into the PstI and *PacI* sites in the polylinker of the AAV-genome plasmid *pAM-flex*[44], where we had first changed the *EcoRV* site in the *pAM-flex* polylinker to *PacI*, to give ITR-*cmv* $P_{enhancer/chicken\ \beta\text{-}actin}$-dsRED-mir30-shRNA-*woodchuck post-translational regulatory sequence* (*WPRE*)-*bovine growth hormone polyadenylation signal (pA)*-ITR. These constructs were packed into AAV capsids (see section below).

Generation of AAV TetTag-DREADD transgenes. The TetTag transgene components, *cFos-tTA* and $P_{TRE\text{-}tight}$-hM_3D_q-*mCHERRY*, were placed into two separate AAV transgenes. As a building block, we started with the plasmid *p*AAV-*ITR-*$P_{cmv/\beta\text{-}actin}$-*iCre-2A-Venus-WPRE-pA-ITR*[45]. A *PacI* site was first introduced just upstream of the CMV/β-actin promoter in this plasmid using Quick Change Mutagenesis (Agilent) (Primers 5′-CTG GAA GCT CCT TAA TTA ACG CTC TCC TGT TCC GAC C-3′ and 5′-GGT CGG AAC AGG AGA GCG TTA ATT AAG GAG CTT CCA G-3′), and the "$P_{cmv/\beta\text{-}actin}$-*Cre-2A-Venus*" fragment then removed with *PacI* and *NotI* digestion. To generate the AAV-*cFos-tTA* construct, the *cFos-tTA* cassette, from a plasmid containing a *cFos* promoter/first intron −764/+918 fragment (P_{cFos}) linked to the tTA reading frame[24] (Addgene plasmid 34856; gift from M. Mayford, Scripps Research Institute), was PCR-amplified (the forward primer with a *NotI* site: 5′-GCATTCCACCACTGCGGCCGCTC ATCAGTTCCATAGG-3′ and reverse primer with a PacI site: 5′-GGTGCGG GCCTCTTCTTCTTAATTAAGCCAGACGGCCGCAGC-3′) and subcloned into the *PacI/NotI* digested Cre-Venus vector, to give *p*AAV-*ITR-*P_{cFos}-*tTA-WPRE-pA-ITR*; For the generation of the pAAV-*ITR-*$P_{TRE\text{-}tight}$-hM_3D_q-*mCherry-WPRE-pA-ITR* construct, we started with the plasmid *p*AAV-*hSyn-double floxed* hM_3D_q-*mCHERRY*[46] (a gift from Bryan L. Roth, University of North Carolina; Addgene plasmid 44361), which contains an inverted hM_3D_q-*mCherry* reading frame flanked by *AscI* and *NheI* sites. We PCR-amplified (forward primer hM_3D_q-NheI-F: 5′-CGAAGGTTATGGCTAGCCTTACTTGTACAGCTCG-3′; reverse primer hM_3D_q-AscI-R: 5′-CTTTATACGAAGTTATGGGCGCGCCAC CATGAC-3′) the hM_3D_q-*mCHERRY* reading frame (including the Kozak ATG initiation sequence CCATGG), and placed this fragment back in the *NheI/AcsI* digested parent plasmid, but now in the sense orientation between the *lox* sites to give "hSyn-double floxed hM_3D_q-mCherry sense". We then removed the *hSyn* promoter from this construct by *MluI* and SalI digestion, and replaced the promoter with the *TRE-tight* ($P_{TRE\text{-}tight}$) promoter; this was PCR-amplified from the *pTRE-Tight* plasmid (Clontech; forward primer, 5′-CTTCACACGCGTTT ACTCCCTATCAGGATAGAG-3′; reverse primer, 5′-CAGCTGACTAGTCGA CCCCCGGGTAC-3′), then digested with *MluI* and SalI. The final construct was pAAV-*ITR-*$P_{TRE\text{-}tight}$-hM_3D_q-*mCHERRY-WPRE-pA-ITR*.

Generation of recombinant AAV particles. All AAV transgenes were packaged into AAV capsids (mixed serotype 1 & 2, 1:1 LORR ratio of AAV1 and AAV2 capsid proteins with AAV2 ITRs)[44,47]. HEK293 cells were co-transfected, using the calcium phosphate method, with AAV transgene plasmid, the adenovirus helper plasmid *pFΔ6*, and the AAV helper plasmids *pH21* (AAV1), and *pRVI* (AAV2)[47]. 60–65 h after transfection, cells were washed in 1xPBS, and pelleted; pellets were resuspended in 150 mM NaCl, 20 mM Tris pH 8.0. Then sodium deoxycholate (Sigma #D5670) and benzonase endonuclease (Sigma #E1014) were added and incubated at 37 °C for 1 h. After incubating, cell debris were removed by centrifugation and AAV particles were purified from the supernatant by passing over a heparin column (1-ml HiTrap Heparin columns, Sigma #5-4836), which binds the AAV particles[47]. The column was pre-equilibrated with 10 ml 150 mM NaCl, 20 mM Tris pH 8.0. Then the supernatant was loaded onto the column at 200 µl/min flow rate; the column was washed with 20 ml 100 mM NaCl, 20 mM Tris pH 8.0 and virus was eluted off the column as follows: 1 ml 200 mM NaCl, 20 mM Tris pH 8.0 (discarded), 1 ml 300 mM NaCl, 20 mM Tris pH 8.0 (discarded), 1.5 ml 400 mM NaCl, 20 mM Tris pH 8.0 (collected), 3 ml 450 mM NaCl, 20 mM Tris pH 8.0 (collected), 1.5 ml 500 mM NaCl, 20 mM Tris pH 8.0 (collected). After purification, AAV particles were concentrated using AMICON ULTRA-4 (100000MWCO; Millipore; CatNo. UFC810024) at 2,000*g* for 10 min. The concentrator was twice refilled with 3.5 ml of 0.9% NaCl (wt/vol). Elutions were removed to a sterile tube, and 250 µl of 0.9% NaCl were added. AAV was aliquotted and stored at −80 °C.

Mice. All experiments were performed in accordance with the United Kingdom Home Office Animal Procedures Act (1986), and had local ethical approval. All the knockdown and TetTag-DREADD experiments used adult male C57BL/6 mice, 8–12 weeks old, purchased from Harlan UK. The $Vgat^{lox/lox}$ mice[33] were purchased from JAX labs (stock no. 012897; donated by Bradley Lowell). Mice were kept on a 12:12 light:dark cycle, at a maximum of four animals per cage, with free access to food and water. Behavioral experiments, except where specified otherwise, were performed during "lights-off".

Stereotaxic injections of AAV. Mice were anesthetized with 2% isoflurane (vol/vol) in O_2 by inhalation and mounted into a stereotaxic frame (Angle two, Leica Microsystems) linked to a digital mouse brain atlas. Mice were maintained on 1.5–2% isoflurane during the surgery. Mice that had been injected with AAVs were allowed 1 month to recover and for the viral transgenes to adequately express before undergoing behavioral experiments.

LC injections of *shAdra2a1* and *shAdra2a2* and *shscramble* AAVs. The AAVs to target the LC were injected into separate cohorts of adult C57BL/6 mice using 0.5–1 µl of virus, plus 0.5 µl 20% mannitol (wt/vol) to increase injection spread[48], at 0.1 µl/min controlled by an ultramicropump (World Precision Instruments), using pre-calibrated pulled glass pipettes with a tip diameter of 6–10 µm. Coordinates, measured in millimeter from Bregma were: −5.4 AP, ± 0.8 ML, −3.7 DV.

Preoptic hypothalamic injections of TetTag-DREADD and Cre-2A-Venus AAVs. The two TetTag-DREADD AAVs (AAV-P_{cFos}-*tTA* and AAV-$P_{TRE\text{-}tight}$-hM_3D_q-*mCHERRY*) were premixed in an equal ratio. AAV injections were done into adult C57BL/6 mice, with 0.5 µl of AAV mixture plus 0.5 µl 20% mannitol (total 1 µl volume). All injections used a 10 µl Hamilton syringe at a rate of 0.25 µl/min. The AAV-*Cre-2A-Venus* transgene[45] (gift from T. Kuner, University of Heidelberg) was packaged into AAV capsids (see above) and 0.5 µl AAV and 0. 5 µl mannitol (20%) injected into adult $Vgat^{lox/lox}$ mice. AAVs were injected bilaterally into the

© 2015 Nature America, Inc. All rights reserved.

doi:10.1038/nn.3957

LPO (AP +0.2 mm, ML ± 0.75 mm, DV −5.7 mm relative to Bregma), or with one injection into MnPO (AP +0.4 mm, ML 0 mm, DV −4.5 mm relative to Bregma), or bilateral injections into the superior colliculi (AP −3.8 mm, ML ± 1.0 mm, DV −2.0 mm relative to Bregma).

Fitting of Neurologgers. Mice were chronically implanted with skull screw electrodes (−1.5 mm Bregma, +1.5 mm midline – first recording electrode; +1.5 mm Bregma, −1.5 mm midline – second recording electrode; −1 mm Lambda, 0 mm midline – reference electrode) to measure cortical EEG and the electrical signals were recorded on a wireless electronic recording device (Neurologger 2) as described previously[43,49].

Assay for sedation. 50 to 100 µg per kg of dexmedetomidine (Tocris Bioscience), dissolved in saline was delivered intraperitoneally and animals, fitted with Neurologgers, were placed immediately afterwards in the activity cage for 15 min to assess locomotor activity (Med Associates Activity Monitor Version 5 for mice). The EEG of animals was simultaneously recorded.

Assay for LORR. 400 µg per kg of dexmedetomidine was delivered intraperitoneally and animals, fitted with Neurologgers, were placed in a continuously slowly rotating cylinder[43]. A rotation rate of 3 rpm was found to give a robust and reproducible LORR in control mice[43]. Animals were scored as positive for LORR if they had rolled onto their backs in the rotating cylinder and made no obvious attempt to right themselves for at least 60 s. The EEG of animals was simultaneously recorded.

TetTag-pharmacogenetic behavioral protocols. After AAV injection, mice were raised on food with 40 mg per kg doxycycline (Harlan TD.120240 40 ppm Doxycycline Diet 2018B) for four weeks[24]. For the behavioral experiments to examine dexmedetomidine-induced sedation, dexmedetomidine or saline i.p. injection took place 48 h after removal of doxycycline. We chose this time point because it gave the optimum ratio of basal vs. induced transgene expression. At the end of the sedation experiments, mice were then put back on the doxycycline diet (Harlan TD 09295 1000 ppm Doxycycline Diet 2018). 4 d after dexmedetomidine-induced sedation, clozapine-N-oxide (C0832, Sigma-Aldrich, dissolved in saline, 5 mg per kg) was injected i.p. into TetTag-DREADD mice fitted with Neurologger2 devices. All CNO and dexmedetomidine injections were carried out during "lights off". 30 min after CNO injection, behavior was assessed in the activity cage as described above.

Sleep deprivation and recovery sleep. Sleep deprivation started 2 d after removal of doxycycline and started at Zeitgeber time zero. The control group was allowed normal sleep; the experimental group was sleep deprived for 4 h by introducing novel objects or tapping lightly on the cages[50]. To reduce the possibility of stress, we never touched the mice directly. Mice were then placed back into their home cages where they exhibited strong and sustained recovery NREM sleep. CNO (5 mg per kg) responses were examined four days from the recovery. At the end of the sleep recovery day, mice were put back on food with 1 g per kg doxycycline (or 1 g/l doxycycline in the drinking water), which was replaced with 40 mg per kg doxycycline the following day[24].

EEG analysis. Four data channels could be recorded at a sampling rate of 200 Hz and were low-pass filtered with a cut-off at 1 Hz (−3 db). The EEG data recorded by the Neurologger2 devices were downloaded and waveforms visualized using Spike2 software (Cambridge Electronic Design) or MATLAB (MathWorks). EEG data were analyzed using Fourier transforms to average power spectra over time[43]. The power spectra were normalized such that the total area under the spectra for the saline controls was unity.

Measurement of body temperature. The body temperature of the mice was recorded using a miniature data logger (DSTnano; Star-Oddi) that was implanted seven days previously in the peritoneal cavity. The loggers were programmed to record every 30 min during 24-h sleep recordings, every 5 min during sleep deprivation and recovery sleep, or every 2 min for experiments with dexmedetomidine or CNO injection. The loggers were recovered and the data downloaded at the end of the experiments.

Adra2a mRNA levels. Locus coeruleus *Adra2a* mRNA levels were determined from adra2a KD and scramble AAV-injected mice by real time qPCR ($n = 4$), using a Taqman RNA-to-CTTM1-Step kit (Applied Biosystems). Briefly, brains were removed and 1-mm tissue punches were collected using 1-mm interval mouse brain matrix (Zivic Instruments) and 1-mm core diameter hollow needles. Total RNA was extracted from frozen tissues using TRIzol. qPCR was performed on an ABI StepOne Plus Real Time PCR system (Applied Biosystems) using the *Adra2a* primers (Applied Biosystems, Mm00845983_s1), described previously[43]. Data were evaluated with SDS 2.1 software, using the Comparative CT method (ΔΔCT) to measure gene expression. Relative expression of the *Adra2a* mRNA was determined by comparing AAV-shRNA mRNA levels in the knockdown group to those in AAV-scramble, mice and normalized to expression of tyrosine hydroxylase (TH) mRNA (TH primers were: Applied Biosystems, Mm00447557_m1).

Immunohistochemistry (fluorescent detection). Adult mice were anesthetized, transcardially perfused with 4% paraformaldehyde (wt/vol) in PBS, pH 7.4. Brains were removed and 40-µm-thick coronal sections cut using a Leica VT1000S vibratome. Free-floating sections were washed in PBS three times for 10 min, permeabilized in PBS plus 0.4% Triton X-100 (vol/vol) for 30 min, blocked by incubation in PBS plus 4% normal goat serum (NGS, vol/vol), 0.2% Triton X-100 for 1 h (all at 22 ± 2 °C) and subsequently incubated with a cFOS monoclonal antibody[29] (1:10,000, Santa Cruz Biotechnology, CatNo.sc-253), and/or a *mCHERRY* monoclonal antibody (1:2,000, Clontech, CatNo.632543), or a tyrosine hydroxylase monoclonal antibody (1:1,000, Sigma T-2928), or with GFP antiserum (1:1,000, Life Technology, A6455)[44]. Primary antisera were diluted in PBS plus 2% NGS overnight at 4 °C. Incubated slices were washed three times in PBS plus 1% NGS for 10 min at 22 ± 2 °C, incubated for 2 h at 22 ± 2 °C with a 1:1,000 dilution of a Alexa Fluor 488 goat anti-rabbit IgG (H+L) (1:1,000, Molecular Probes, CatNo.A11034) and Alexa Flour 594 goat anti-mouse IgG (H+L) (1:1,000, Molecular Probes, CatNo.A11005) in PBS plus 1% NGS, and subsequently washed there times in PBS for 10 min at 22 ± 2 °C. The sections were mounted on slides and coverslipped. Antibody validation: The cFOS antibody gave selective nuclear neuronal staining following an excitatory stimulus in a pattern consistent with many other studies (for example, refs. 21 and 31) and staining with this antibody also mimicked the induction of the *cFos* promoter-based TetTag transgenes, further indicating specificity; the mCHERRY monoclonal antibody did not stain brain sections unless the area had been transduced with an AAV expressing the hM_3D_q-mCHERRY fusion protein; the tyrosine hydroxylase monoclonal antibody selectively stained neurons in the locus ceruleus, consistent with the known restricted expression of the tyrosine hydroxylase gene.

Immunohistochemistry (diaminobenzidine staining). We used DAB staining to better visualize nuclear cfos expression over a relatively large area. 30 min after i.p. dexmedetomidine (50, 100, 400 µg per kg), or saline (0.9%, wt/vol) administration, experimental mice were anesthetized, perfused transcardially, and free-floating sections processed for immunohistochemistry with rabbit antibody to Fos[29] (1:20,000, Ab-5, Calbiochem) after blocking endogenous peroxidase with 0.3% H_2O_2 (vol/vol) in PBS. The primary antiserum was localized using a variation of the avidin-biotin complex system (Vector Laboratories). In brief, sections were incubated for 120 min at 22–25 °C in a solution of biotinylated goat anti-body to rabbit IgG (PK-6101, Vector Laboratories) and then placed in the mixed avidin-biotin horseradish peroxidase complex solution (ABC Elite Kit, Vector Laboratories) for 60 min. The peroxidase complex was visualized by a 4 to 5-min exposure to chromogen solution (0.05% 3,30-diaminobenzidine tetrahydrochloride (wt/vol, Sigma-Aldrich), 0.4 mg/ml nickel ammonium sulfate to produce a blue-black product. The reaction was stopped by washing in distilled water and PBS. Sections were dehydrated and coverslipped with quick mounting medium (Eukitt, Fluka Analytical).

Electrophysiology and single-cell qPCR. For acute brain slice recordings of LPO and LC neurons, 250 µm-sections were cut with a Vibratome (Campden Instruments) in ice-cold slicing solution containing (in mM): 85 NaCl, 2.5 KCl, 1 $CaCl_2$, 4 $MgCl_2$, 1.25 NaH_2PO_4, 26 $NaHCO_3$, 75 sucrose, 25 glucose, pH 7.4 when bubbled with 95% O_2 and 5% CO_2. After incubating in slicing solution for 15–30 min at 22 ± 2 °C, slices were then transferred to oxygenated ACSF containing (in mM): NaCl 125, KCl 2.5, $CaCl_2$ 2, $MgCl_2$ 1, NaH_2PO_4 1.25,

© 2015 Nature America, Inc. All rights reserved.

$NaHCO_3$ 26, glucose 11. For the LC recordings, the solution also contained 1 mM kynurenic acid. For whole-cell current clamp recordings, patch pipettes (4–6 MΩ) were backfilled with internal solution containing (in mM): 145 K-gluconate, 4 NaCl, 5 KCl, 0.5 $CaCl_2$, 5 EGTA, 10 HEPES, 4 Mg-ATP, 0.3 Na-GTP, and 10 sucrose, pH 7.3, adjusted with KOH for the LPO recordings and (in mM) 130 KCl, 10 HEPES, 0.1 BAPTA, 5 $MgCl_2$, 3 Na_2-ATP, 0.1 Na-GTP, 8 phosphocreatine, pH 7.3 for the LC recordings[29].

For single-cell qPCR, after achieving a whole-cell recording the content of the neuron was aspirated under visual control into the recording pipette and expelled into single cell lysis/DNAseI solution using the Single-Cell-to-CT Kit (Ambion). Reverse transcription, cDNA pre-amplification and qPCR were performed following the manufacturer's guidelines using the TaqMan Gene Expression Assay system (Applied Biosystems, Foster City, USA). The primer reference numbers were: *hprt*: Mm01545399_m1; *gad1*: Mm04207432_g1; *gad2*: Mm00484623_m1; *vglut1*: Mm00812886_m1; *vglut2*: Mm00499876_m1.

Statistical analyses. Prism6 and Origin were used for statistical analysis. No statistical methods were used to predetermine sample sizes, but our sample sizes are similar to those reported in previous publications (refs. 16,29,31). Data collection and processing were randomized or performed in a counter-balanced manner. Normality was tested by the Shapiro-Wilk test. Equal variances were assessed by F-test. Data are represented as the mean ± s.e.m. For qPCR, LORR and cFOS immunohistochemistry, Fisher's exact test or a two-tailed unpaired *t*-test was performed. For the dexmedetomidine sedation and DREADD behavioral experiments, two-way ANOVA was performed. $P < 0.05$ was considered significant ($^*P < 0.05$, $^{**}P < 0.01$, $^{***}P < 0.001$). Mice were excluded from the analysis if the histology did not confirm significant mCHERRY expression in LPO or MnPO, or if the EEG/EMG recording technology failed during the experiment. In the *Adra2a* knockdown experiments (**Fig. 1**) and *Vgat* deletion experiments (**Fig. 7**), mice brains that had undetectable AAV transgene expression, or with expression beyond the target region, were excluded from the statistics. All the experiments were performed and analyzed blind to treatment conditions.

A **Supplementary Methods Checklist** is available.

43. Gelegen, C. *et al.* Staying awake—a genetic region that hinders alpha adrenergic receptor agonist-induced sleep. *Eur. J. Neurosci.* **40**, 2311–2319 (2014).
44. Murray, A.J. *et al.* Parvalbumin-positive CA1 interneurons are required for spatial working but not for reference memory. *Nat. Neurosci.* **14**, 297–299 (2011).
45. Tang, W. *et al.* Faithful expression of multiple proteins via 2A-peptide self-processing: a versatile and reliable method for manipulating brain circuits. *J. Neurosci.* **29**, 8621–8629 (2009).
46. Krashes, M.J. *et al.* Rapid, reversible activation of AgRP neurons drives feeding behavior in mice. *J. Clin. Invest.* **121**, 1424–1428 (2011).
47. Klugmann, M. *et al.* AAV-mediated hippocampal expression of short and long Homer 1 proteins differentially affect cognition and seizure activity in adult rats. *Mol. Cell. Neurosci.* **28**, 347–360 (2005).
48. Mastakov, M.Y., Baer, K., Xu, R., Fitzsimons, H. & During, M.J. Combined injection of rAAV with mannitol enhances gene expression in the rat brain. *Mo. Ther.* **3**, 225–232 (2001).
49. Vyssotski, A.L. *et al.* EEG responses to visual landmarks in flying pigeons. *Curr. Biol.* **19**, 1159–1166 (2009).
50. Gerashchenko, D. *et al.* Identification of a population of sleep-active cerebral cortex neurons. *Proc. Natl. Acad. Sci. USA* **105**, 10227–10232 (2008).

© 2015 Nature America, Inc. All rights reserved.